

# On the possibility of mixed helical p-wave pairings in $\text{Sr}_2\text{RuO}_4$

Wen Huang<sup>1,\*</sup> and Zhiqiang Wang<sup>2,†</sup>

<sup>1</sup>*Shenzhen Institute for Quantum Science and Engineering & Guangdong Provincial Key Laboratory of Quantum Science and Engineering, Southern University of Science and Technology, Shenzhen 518055, Guangdong, China*

<sup>2</sup>*James Franck Institute, University of Chicago, Chicago, Illinois 60637, USA*

(Dated: November 3, 2021)

The exact nature of the unconventional superconductivity in  $\text{Sr}_2\text{RuO}_4$  remains a mystery. At the phenomenological level, no superconducting order parameter proposed thus far seems able to coherently account for all of the essential experimental signatures. One prominent observation is the polar Kerr effect, which implies an anomalous Hall effect. Without appealing to extrinsic factors originating from crystalline imperfection, this peculiar effect may be interpreted as an evidence of a bulk chiral Cooper pairing with nonzero orbital angular momentum, such as  $p + ip$  or  $d + id$ . In this paper, we propose alternative possibilities with complex mixtures of distinct helical p-wave order parameters, namely,  $A_{1u} + iA_{2u}$  and  $B_{1u} + iB_{2u}$  in the group theory nomenclature. These states essentially consist of two copies of inequivalent chiral p-wave pairings with opposite chirality and different pairing amplitudes, and therefore support intrinsic Hall and Kerr effects. We further show that these states exhibit salient features which connect to several other key observations in this material, including the absence of spontaneous current, a substantial Knight shift drop, and possibly signatures in uniaxial strain and ultrasound measurements.

The nature of the unconventional superconductivity in  $\text{Sr}_2\text{RuO}_4$  is an outstanding puzzle [1–10]. Its normal state properties have been characterized with unprecedented accuracy — an incredible feat that is not often seen in other unconventional superconductors. The electron correlation in this material is moderate, and superconductivity emerges out of a well-behaved Fermi liquid [3]. These have led to a popular perception that resolving its pairing mechanism and identifying its pairing symmetry should be well within the capacity of established theories and experimental techniques. Yet, despite tremendous efforts over the past twenty plus years, neither of these two key issues has been settled. This is largely due to the lack of an order parameter that could coherently interpret all the essential experimental observations [9, 10].

Arguably, one principal property of the superconductivity in  $\text{Sr}_2\text{RuO}_4$  is the condensation of at least two superconducting order parameters. This has been inferred from a variety of experiments, including  $\mu\text{SR}$  [11, 12], optical polar Kerr effect [13], Josephson interferometry [14], and ultrasound [15, 16], etc. A multi-component pairing is realized if the Cooper pairing is developed in a multi-dimensional irreducible representation (irrep) of the crystal point symmetry group. One notable example is the chiral p-wave pairing, i.e.  $(k_x + ik_y)\hat{z}$ , which belongs to the  $E_u$  irrep of the  $D_{4h}$  group. Here,  $\hat{z}$  denotes the orientation of the so-called  $\mathbf{d}$ -vector, which describes the spin configuration of a spin-triplet pairing [3]. Another possibility is coexisting order parameters associated with distinct one-dimensional irreps. In this scenario, the multiple components typically condense below distinct critical temperatures, although accidental near-degeneracy is possible, in principle.

In light of the evidence of time-reversal symmetry breaking from the  $\mu\text{SR}$  and the polar Kerr effect measurements [11–13], the multiple components presumably form a complex pairing, such that the state does not return to itself after a time-reversal operation. The Kerr effect, and the closely re-

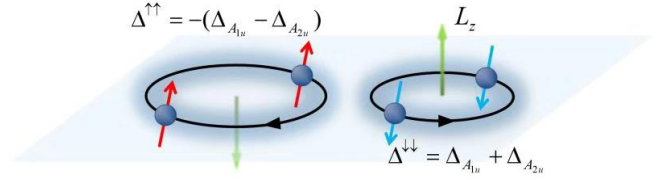


Figure 1. (color online) Illustration of the Cooper pairing in the mixed helical p-wave  $A_{1u} + iA_{2u}$  state in a single-orbital model. The state consists of two copies of chiral p-wave model with opposite chirality. The Cooper pairs are drawn with different size to reflect their different pairing amplitudes. Green arrows indicate the direction of the Cooper pair orbital angular momentum  $L_z$ . In the limit  $\Delta_{A_{1u}} = \Delta_{A_{2u}}$ , the state resembles the  $^3\text{He}$   $A_1$ -phase. Another candidate state  $B_{1u} + iB_{2u}$  has a similar pairing configuration.

lated anomalous Hall effect, intuitively imply an underlying chiral pairing with nonzero orbital angular momentum, such as  $p + ip$  and  $d + id$ , as is substantiated by a recent study [17]. Hence, if the Kerr effect in this material is intrinsic (i.e. not related to extrinsic effects such as impurities or lattice dislocations), its superconducting symmetry is limited to a few candidates.

In this work, we turn to the helical p-wave pairings ( $A_{1u}$ ,  $A_{2u}$ ,  $B_{1u}$  and  $B_{2u}$  irreps), which are analogues of the  $^3\text{He}$  B-phase [18]. They individually preserve time-reversal symmetry, as each effectively consists of a pair of sub-Hilbert space characterized respectively by  $k_x + ik_y$  and  $k_x - ik_y$  pairings with identical gap amplitude. However, appropriate complex mixture of these helical pairings could tune the relative gap amplitude between  $k_x + ik_y$  and  $k_x - ik_y$  away from unity (see Fig. 1). The resultant ‘asymmetric’ state then supports intrinsic Kerr effect. We are mainly interested in the scenarios of two-component order parameters, for which we identify two possibilities that meet our requirement:  $A_{1u} + iA_{2u}$  and  $B_{1u} + iB_{2u}$ . The idea is most transparent when presented in a single-orbital model. Take the former as an example, in

terms of the  $\mathbf{d}$ -vector, the pairing functions of  $A_{1u}$  and  $A_{2u}$  are given respectively by  $k_x\hat{x} + k_y\hat{y}$  and  $k_x\hat{y} - k_y\hat{x}$ . The full gap function then becomes,

$$\mathbf{d}_{\mathbf{k}} = \Delta_{A_{1u}}(k_x\hat{x} + k_y\hat{y}) + i\Delta_{A_{2u}}(k_x\hat{y} - k_y\hat{x}), \quad (1)$$

where  $\Delta_{A_{1(2)u}}$  are real gap amplitudes.  $\mathbf{d}_{\mathbf{k}}$  is non-unitary since  $\mathbf{d}_{\mathbf{k}}^* \times \mathbf{d}_{\mathbf{k}} \neq 0$  [18], implying unequal pairing gap amplitudes for the two spin species:  $\Delta^{\uparrow\uparrow}(\mathbf{k}) = -(\Delta_{A_{1u}} - \Delta_{A_{2u}})(k_x - ik_y)$  for spin-up and  $\Delta^{\downarrow\downarrow}(\mathbf{k}) = (\Delta_{A_{1u}} + \Delta_{A_{2u}})(k_x + ik_y)$  for spin-down (Fig. 1). If  $\Delta_{A_{1u}} = \Delta_{A_{2u}}$ , the state resembles the  $^3\text{He } A_1$ -phase which has one spin component unpaired [18]. More generally, both spin species are paired and they carry opposite orbital chiralities, i.e. opposite  $L_z$ . Such a state is odd-parity by nature [21], and it exhibits other salient features potentially consistent with the absence of spontaneous current signature [23, 24] and the substantial Knight shift drop [19, 20], as we shall see later. Since the  $B_{1u} + iB_{2u}$  state essentially shares the same general features, we will not present further analyses about it in the remaining of the paper.

At this point, it is worth pointing out that multiple microscopic calculations [26–32] have found that helical pairing states are favored in certain reasonable interaction parameter space. More interestingly, in some cases the splitting among various helical states could be rather small [32], making it reasonable to consider accidentally degenerate pairing. Here, we make no attempt to delve upon the pairing mechanism or upon how the pairing is distributed among the multiple orbitals in  $\text{Sr}_2\text{RuO}_4$ . Instead, we will focus on the general phenomena that do not rely on microscopic details. Apart from some occasional general discussions, our analyses will be largely based on a concrete two-orbital model containing the Ru  $d_{xz}$  and  $d_{yz}$  orbitals. As far as the physical properties to be discussed are concerned, we expect the same qualitative features for more general multi-orbital models of  $\text{Sr}_2\text{RuO}_4$ . For simplicity, we assume the simple pairing functions for the various odd-parity (p-wave) superconducting channels as given in Table I.

Table I. Representative simple odd-parity pairing gap functions ( $\mathbf{d}$ -vectors) for the two-orbital model containing the Ru  $d_{xz}$  and  $d_{yz}$  orbitals.

irrep	$\mathbf{d}_{xz}$	$\mathbf{d}_{yz}$
$A_{1u}$	$\sin k_x\hat{x}$	$\sin k_y\hat{y}$
$A_{2u}$	$\sin k_x\hat{y}$	$-\sin k_y\hat{x}$
$B_{1u}$	$\sin k_x\hat{x}$	$-\sin k_y\hat{y}$
$B_{2u}$	$\sin k_x\hat{y}$	$\sin k_y\hat{x}$
$E_u$	$\sin k_x\hat{z}$	$\sin k_y\hat{z}$

## AC ANOMALOUS HALL EFFECT AND KERR ROTATION

Since our proposed state is essentially composed of a pair of (spinless) chiral p-wave models with opposite chirality and inequivalent gap amplitudes, we expect it to support anomalous Hall effect. Notably, while the intrinsic anomalous Hall

effect is generally absent in single-orbital chiral superconducting models [33–36],  $\text{Sr}_2\text{RuO}_4$  has an inherent multi-orbital character.

Below we demonstrate intrinsic a.c. anomalous Hall effect and Kerr rotation for the  $A_{1u} + iA_{2u}$  state, using the same two-orbital model as in Ref. [34]. Without qualitative impacts on our results, we neglect spin-orbit coupling (SOC) in this section for simplicity. Then the spin up and down blocks decouple and their contributions to the two-dimensional Hall conductivity  $\sigma_H$  can be computed separately. Here, we briefly describe the spin up block of the model. Written in the basis  $(c_{d_{xz},\uparrow}(\mathbf{k}), c_{d_{yz},\uparrow}(\mathbf{k}))$ , where  $c_{d_{xz},\uparrow}$  and  $c_{d_{yz},\uparrow}$  are annihilation operators for the  $d_{xz}$  and  $d_{yz}$  orbitals of  $\text{Sr}_2\text{RuO}_4$ , the normal state Hamiltonian reads,

$$H_N(\mathbf{k}) = \begin{pmatrix} \xi_{xz}(\mathbf{k}) & \lambda(\mathbf{k}) \\ \lambda(\mathbf{k}) & \xi_{yz}(\mathbf{k}) \end{pmatrix}, \quad (2)$$

where  $\xi_{xz}(\mathbf{k}) = -2t \cos k_x - 2\tilde{t} \cos(k_y) - \mu$ ,  $\xi_{yz}(\mathbf{k}) = -2\tilde{t} \cos k_x - 2t \cos(k_y) - \mu$ ,  $\lambda(\mathbf{k}) = 4t' \sin k_x \sin k_y$ . Here  $t$  labels the nearest neighbor hopping integral of the  $d_{xz(yz)}$  orbital along the  $x(y)$  direction,  $\tilde{t}$  that of the  $d_{xz(yz)}$  orbital along the  $y(x)$  direction,  $t'$  denotes the hybridization of the two orbitals between next nearest neighboring sites. The corresponding BdG Hamiltonian follows as,

$$H_{\text{BdG}}^{\uparrow}(\mathbf{k}) = \begin{pmatrix} H_N(\mathbf{k}) & \hat{\Delta}_{\uparrow\uparrow}(\mathbf{k}) \\ \hat{\Delta}_{\uparrow\uparrow}^{\dagger}(\mathbf{k}) & -H_N^T(-\mathbf{k}) \end{pmatrix}, \quad (3)$$

where, following Table I,

$$\hat{\Delta}^{\uparrow\uparrow}(\mathbf{k}) = -(\Delta_{A_{1u}} - \Delta_{A_{2u}}) \begin{pmatrix} \sin k_x & 0 \\ 0 & -i \sin k_y \end{pmatrix}. \quad (4)$$

Using  $H_{\text{BdG}}^{\uparrow}$  we calculate  $\sigma_H^{\uparrow}(\omega)$  from the standard Kubo formula (without vertex corrections). Details of the calculation can be found in the Supplementary Materials [37]. The same calculation is done for  $\sigma_H^{\downarrow}$  and the numerical result of the total  $\sigma_H$  at temperature  $T = 0$  is presented in Fig. 2. Not surprisingly,  $\sigma_H$  is nonzero; both its real and imaginary parts have similar frequency dependence to those obtained for a chiral p-wave pairing [34]. The overall magnitude of  $\sigma_H$  is reduced by a factor of two for equal or comparable magnitudes of  $\Delta_{A_{1u}}$  and  $\Delta_{A_{2u}}$ , compared to that in Ref. [34], because in the current scenario  $\sigma_H^{\uparrow}$  and  $\sigma_H^{\downarrow}$  partially cancel out each other while the cancellation is absent in the chiral p-wave pairing case.

We note that  $\text{Im}[\sigma_H(\omega)]$  becomes nonzero at  $\omega \gtrsim 0.4 \text{ eV}$  for the chosen band parameters. This frequency is determined by the minimum energy cost to create a pair of Bogoliubov quasiparticles from different bands, which is not dictated by  $2|\Delta^{\uparrow\uparrow}|$  or  $2|\Delta^{\downarrow\downarrow}|$  but by the hopping parameter  $t'$  [34]. Therefore, even though  $|\Delta^{\uparrow\uparrow}|$  and  $|\Delta^{\downarrow\downarrow}|$  can be quite different, the onset frequencies of  $\text{Im}[\sigma_H^{\uparrow}]$  and  $\text{Im}[\sigma_H^{\downarrow}]$  are actually almost identical.

From the calculated  $\sigma_H$  one can estimate the Kerr rotation angle using

$$\theta_K(\omega) = \frac{4\pi}{\omega d} \text{Im}\left[\frac{\sigma_H(\omega)}{n(n^2 - 1)}\right], \quad (5)$$

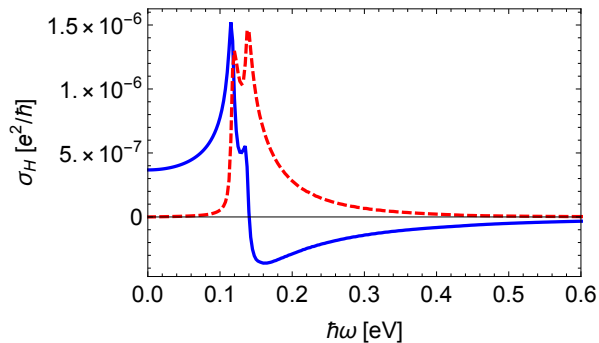


Figure 2. (color online) Real (blue solid line) and imaginary (red dashed line) parts of the  $\sigma_H(\omega)$  as a function of  $\omega$  at  $T = 0$ . Band parameters are [34]:  $t = \mu = 0.4$  eV,  $t' = 0.05t$  and  $\tilde{t} = 0.1t$ .  $\Delta_{A_{1u}} = 2\Delta_{A_{2u}} = \frac{2}{3}\Delta_{\max}$  with  $\Delta_{\max} = |\Delta_{A_{1u}}| + |\Delta_{A_{2u}}| = 0.23$  meV [34]. We choose  $|\Delta_{A_{1u}}| \neq |\Delta_{A_{2u}}|$  so that the gap magnitudes are nonzero for both spin up and down; otherwise, one spin component would remain normal at zero temperature which is not observed.

where  $n = n(\omega)$  is the complex index of refraction and  $d$  is the interlayer spacing of  $\text{Sr}_2\text{RuO}_4$  along the  $c$ -axis.  $n(\omega)$  can be estimated from the longitudinal optical conductivity which is modeled by a Drude model as in Ref. [34]. For details see Ref. 37. The estimated  $\theta_K(\hbar\omega = 0.8$  eV)  $\approx 20$  nrad [37], which may potentially account for the experimental value of 65 nrad observed by J. Xia *et al* [38], given the uncertainty in our estimate of  $n(\omega)$  as well as the neglecting of the  $\gamma$  band in the current calculation. We note that  $\sigma_H$ , and therefore the estimated Kerr angle  $\theta_K$ , does depend on the actual ratio between  $|\Delta_{A_{1u}}|$  and  $|\Delta_{A_{2u}}|$ . However, the dependence is quite weak as long as the two are comparable [37].

## SPONTANEOUS CURRENT

A chiral p-wave state shall generate finite spontaneous surface current [39, 40]. Following the original proposal of chiral p-wave pairing in  $\text{Sr}_2\text{RuO}_4$ , attempts to detect signatures of such a current have had little success, suggesting that the spontaneous current is either simply absent or too tiny to be resolved in actual measurements [23, 24].

The  $A_{1u} + iA_{2u}$  state has just the right appeal for explaining this, which is already obvious in the single-orbital case. Here, the two spin species each generates an edge current, and these currents flow in opposite direction due to the opposite chirality. Moreover, the integrated current in fact vanishes in the BCS limit. However, thanks to the distinct decay length scales of the two contributions, the current distribution does not exactly cancel at each spatial point.

Going beyond single-orbital model, the integrated current may not vanish due to SOC and other band structure effects. However, the strong suppression persists, as is demonstrated in Fig. 3 for our two-orbital model. Neglecting the fast Friedel oscillations, the spontaneous current generally contains two canceling contributions characterized by different

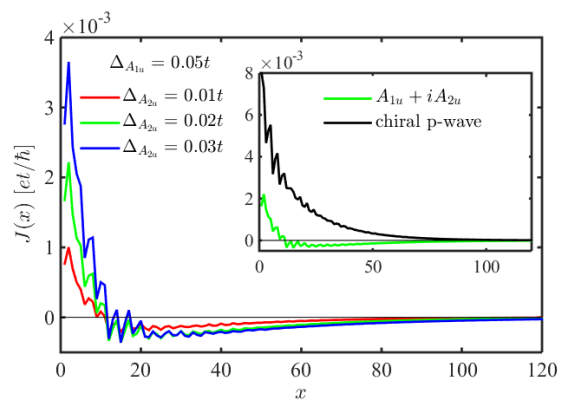


Figure 3. (color online) Distribution of zero-temperature spontaneous edge current in our two-orbital model with a mixed helical p-wave  $A_{1u} + iA_{2u}$  pairing on the quasi-1D  $d_{xz}$  and  $d_{yz}$  orbitals. The  $A_{1u}$  component is held fixed at  $\Delta_{A_{1u}} = 0.05t$ . Inset: a comparison of the spontaneous current in the mixed helical and chiral p-wave phases with similar gap amplitudes. These calculations follow those in Refs. [42, 43], and lattice constant is defined to be unity.

decay length scales. For the calculations shown in the figure, the net current in the mixed helical state is typically more than twenty times smaller than that in a chiral p-wave state with similar gap magnitudes (See inset of Fig. 3).

It should be stressed that such suppression is inherent, as it is achieved without appealing to surface disorder, anisotropic band and gap structure — factors typically having the potential to further reduce the spontaneous current, as is known for the case of chiral p-wave [41–46]. In fact, this behavior is also expected from the Ginzburg-Landau theory, at the lowest order of which the spontaneous current is related to cross-gradient bilinears of the involving order parameters, such as  $\partial_x \Delta_{A_{1u}}^* \partial_y \Delta_{A_{2u}}$  [45, 47]. In the present case, this lowest order contribution vanishes by symmetry, and higher order terms such as  $\partial_x^3 \Delta_{A_{1u}}^* \partial_y \Delta_{A_{2u}}$  are needed to account for the small local current distribution. By the same token, similar physics occurs for the chiral  $d_{x^2-y^2} + id_{xy}$  pairing [48]. In passing, we note that for the  $B_{1g} + iA_{2g}$  state [49], i.e. the  $d_{x^2-y^2} + ig_{xy}(x^2-y^2)$  pairing, the spontaneous current is in general finite at the (100) surfaces and vanishes at the (110) surface, analogous to the situation in  $s + id_{xy}$  pairing [40].

Finally, the suppression in the  $A_{1u} + iA_{2u}$  phase is also independent of the edge orientation, and the same phenomenology takes place at the domain walls separating regions of time-reversed pairings.

## SPIN SUSCEPTIBILITY AND KNIGHT SHIFT

Recent revised NMR measurements under external in-plane magnetic field reveal a substantial Knight shift drop below  $T_c$  [19, 20]. This implies a drop of spin susceptibility,  $\chi_{\text{spin}}$ , which was subsequently confirmed by a polarized neutron scattering study [50]. A latter NMR study further places an

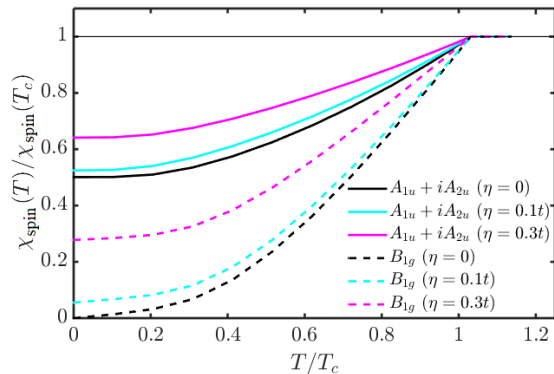


Figure 4. (color online) Temperature dependence of the spin susceptibility in the  $A_{1u} + iA_{2u}$  (solid curves) and  $B_{1g}$  (dashed curves) superconducting states, in the presence of a small Zeeman field in the  $x$ -direction. Here,  $\eta$  denotes the strength of SOC.

upper bound of 10% the normal state susceptibility at the low temperatures [25]. These reports are most straightforwardly explained in terms of spin-singlet pairing. However, as the observed Knight shift contains contributions from both spin and orbital degrees of freedom, the exact fraction of the spin susceptibility drop in the zero field limit may deserve a more careful inquiry [10]. As we argue below, our proposed states may still have the potential to reconcile with the susceptibility drop.

Owing to the in-plane  $\mathbf{d}$ -vector orientation, the mixed helical states naturally exhibit a reduced  $\chi_{\text{spin}}$  across  $T_c$  under the in-plane field. In fact, in the absence of SOC,  $\chi_{\text{spin}}(T = 0)$  equals to half of that in the normal state. This is demonstrated in Fig. 4, which shows the temperature-dependent susceptibility in the presence of a weak Zeeman field directed along the  $x$ -direction. For comparison, we also show results for a spin-singlet  $d$ -wave state (a pairing in the  $B_{1g}$  irrep). In the calculations, we have assumed that the two helical pairings onset at the same critical temperature, and that their temperature dependence follows the standard BCS mean-field behavior.

The SOC may facilitate extra spin-flipping processes that could have been otherwise suppressed by Cooper pairing, thereby alleviating the drop of  $\chi_{\text{spin}}$ . This is exemplified by the noticeable increase of  $\chi_{\text{spin}}(T = 0)$  as SOC becomes stronger (Fig. 4). Notably, even a pure spin-singlet pairing may develop a residual  $\chi_{\text{spin}}(T = 0)$  [29, 31]. For the two-orbital model in question, this can be explained in the following terms. Here, SOC takes the form of  $\eta \hat{L}_z \hat{s}_z$  where  $\hat{L}_z$  operates on the orbital degrees of freedom and  $\hat{s}_z$  is the Pauli matrix. The SOC term flips the in-plane spin components but not the one along  $z$ . As a consequence, upon turning on a finite  $\eta$ , the  $z$ -component of the spin susceptibility  $\chi_{\text{spin}}^{zz}$  remains fully suppressed at  $T = 0$  (not shown in Fig. 4), whereas the  $x$ -component,  $\chi_{\text{spin}}^{xx}$ , acquires a residual value. We expect such an enhancement of  $\chi_{\text{spin}}(T = 0)$  due to SOC to persist in a more general multi-orbital model of  $\text{Sr}_2\text{RuO}_4$  [51–53]. Finally, it is worth remarking that, the natural mixing

of (real)-spin triplet and singlet pairings in the presence of SOC [51, 54], which is not considered here, may also introduce corrections to the spin susceptibility.

Note that our calculations were done in the non-interacting limit. Correlations renormalize the normal and superconducting state  $\chi_{\text{spin}}$  in different manners, reducing the ratio  $\chi_{\text{spin}}(T = 0)/\chi_{\text{spin}}(T = T_c)$  from its non-interacting value [55]. Based on an estimate of the Wilson ratio of 2 [20, 56] and using the data for  $\eta = 0.1t$  in Fig. 4, we obtain  $\chi_{\text{spin}}(T = 0)/\chi_{\text{spin}}(T = T_c) \approx 35\%$  for the  $A_{1u} + iA_{2u}$  state. This is a substantial overall suppression, although, at face value, still noticeably higher than the upper bound of 10% suggested by the most recent NMR measurement [25]. However, our crude approximation could be insufficient for a quantitative comparison, and a calculation based on a more realistic correlated multiorbital model may be needed. We also take note of the potential complications in disentangling the orbital and spin contributions to the Knight shift [10, 57], which could affect the experimental interpretation.

## STRAIN AND ULTRASOUND

Uniaxial strain and ultrasound measurements reveal crucial information about the symmetry of the superconducting order [15, 16, 58]. Most informative among the existing experiments are the ones that probe the coupling between the order parameters and the  $B_{1g}$  ( $\epsilon_{x^2-y^2}$ ) and  $B_{2g}$  ( $\epsilon_{xy}$ ) strains. For our mixed helical state, the leading order coupling has the following form in the Ginzburg-Landau free energy,

$$f_{\text{coupling}} = \sum_i \epsilon_i^2 (\alpha_i |\Delta_{A_{1u}}|^2 + \beta_i |\Delta_{A_{2u}}|^2) \quad (6)$$

where  $i = x^2 - y^2, xy$  for the  $B_{1g}$  and  $B_{2g}$  strains, respectively, and  $\alpha_i (\beta_i)$  are coupling constants. No other order parameter bilinears is present. This free energy has two implications. On the one hand, the mean-field critical temperatures of the two components shall both follow a quadratic dependence on the strain. This seems to agree with the observed behavior in several uniaxial strain measurements [59, 60]. We do note that there is no solid evidence of the expected split transitions in thermodynamic measurements [61, 62], although this could be explained away by arguments unrelated to symmetry [63]. On the other hand, the absence of a linear coupling to  $\epsilon_i$  in Eq. (6) disallows any discontinuity in the shear elastic moduli  $(c_{11} - c_{12})/2$  or  $c_{66}$ . This stands in contrast with recent reports, where a jump in the latter has been observed [15, 16]. Interestingly, a linear coupling to the  $B_{2g}$  strain (associated with  $c_{66}$ ) is possible for mixed  $A_{1u}$  and  $B_{2u}$ , as well as mixed  $A_{2u}$  and  $B_{1u}$  states [32]. This suggests a way to reconcile our proposed order with the ultrasound experiments: the breaking of crystalline rotational symmetry around lattice dislocations can allow the  $B_{1u}$  and/or  $B_{2u}$  order parameters to locally condense against the backdrop of a bulk  $A_{1u} + iA_{2u}$  order, leading to a local mixture of  $A_{1u}$  with  $B_{2u}$  (and/or  $A_{2u}$  with  $B_{1u}$ ) that couples linearly to the  $B_{2g}$  strain.

## CONCLUDING REMARKS

Under the assumption that the observed polar Kerr effect is a genuine response of superconducting  $\text{Sr}_2\text{RuO}_4$  in the clean limit, we proposed that the mixed helical p-wave  $A_{1u} + iA_{2u}$  and  $B_{1u} + iB_{2u}$  states represent faithful alternative candidates to chiral superconducting states. We also discussed how these states may be compatible with several other key measurements. In addition, as shown in a recent study [64], the helical state may also explain the Pauli limiting behavior of the in-plane  $H_{c2}$  and the first order phase transition observed in the  $H - T$  phase diagram at low  $T$  and at  $H$  near  $H_{c2}$  [65, 67]. The most serious challenge for our proposal is probably the substantial Knight shift drop observed. Although we have argued that the latest NMR measurement [25] does not necessarily rule out our mixed helical states, much further work is needed to fully resolve this issue. Also, a full reconciliation with other important observations may require further examination. For example, the presence of gapless excitations [66, 68–71] would place strong constraint on the detailed forms of the p-wave pairings. To this end, we take note of the multitude of possibilities made available by the multiorbital nature of this material [51–53, 72–80].

The mixed helical states we discuss are also expected to exhibit a finite spin polarization in the bulk, resulting a spontaneous bulk magnetization field that may be probed by SQUID type measurements. However, the field scales as  $(\Delta/E_F)^2$ , which may be below the resolution of the existing SQUID techniques [23, 24, 81].

As a final remark, the  $B_{1g} + iB_{2g}$  state (chiral  $d_{x^2-y^2} + id_{xy}$  pairing) also carries the essential features needed to explain the various observations discussed in this work. Alternatively, in a spirit similar to that proposed in Ref. [82], one can consider that one component of the  $B_{1g} + iB_{2g}$  state is favored in the clean limit, while the other component condenses around lattice dislocations. Note that this scenario would naturally conform with the reported nodal line behavior.

## ACKNOWLEDGMENTS

We acknowledge helpful discussions with Weiqiang Chen, Catherine Kallin, Yongkang Luo, Aline Ramires, Thomas Scaffidi and Fuchun Zhang. WH is supported by NSFC under grant No. 11904155 and the Guangdong Provincial Key Laboratory under Grant No. 2019B121203002. ZW acknowledges financial support from the James Frank Institute at the University of Chicago. Computing resources are provided by the Center for Computational Science and Engineering at Southern University of Science and Technology.

---

\* huangw3@sustech.edu.cn

† zqwang@uchicago.edu

- [1] Y. Maeno, H. Hashimoto, K. Yoshida, S. Nishizaki, T. Fujita, J. G. Bednorz, F. Lichtenberg, *Nature (London)* **372**, 532 (1994).
- [2] Y. Maeno, T. M. Rice, and M. Sigrist, *Phys. Today* **54**(1), 42 (2001).
- [3] A. P. Mackenzie and Y. Maeno, *Rev. Mod. Phys.* **75**, 657 (2003).
- [4] C. Kallin and A. J. Berlinsky, *J. Phys. Condens. Matter* **21**, 164210 (2009).
- [5] C. Kallin, *Rep. Prog. Phys.* **75**, 042501 (2012).
- [6] Y. Maeno, S. Kittaka, T. Nomura, S. Yonezawa, and K. Ishida, *J. Phys. Soc. Jpn.* **81**, 011009 (2012).
- [7] Y. Liu and Z. Q. Mao, *Physica C: Superconductivity and its Application*, **514**, 339 (2015).
- [8] C. Kallin and A. J. Berlinsky, *Rep. Prog. Phys.* **79**, 054502 (2016).
- [9] A. P. Mackenzie, T. Scaffidi, C. W. Hicks and Y. Maeno, *NPJ Quantum Materials* **2**, 40 (2017).
- [10] A. J. Leggett and Y. Liu, arXiv:2010.15220.
- [11] G. M. Luke, Y. Fudamoto, K. M. Kojima, M. I. Larkin, J. Merrin, B. Nachumi, Y. J. Uemura, Y. Maeno, Z. Q. Mao, Y. Mori, H. Nakamura, M. Sigrist, *Nature* **394**, 558 (1998).
- [12] V. Grinenko, S. Ghosh, R. Sarkar, J. Orain, A. Nikitin, M. Elenker, D. Das, Z. Guguchia, F. Brückner, M. E. Barber, J. Park, N. Kikugawa, D. A. Sokolov, J. S. Bobowski, T. Miyoshi, Y. Maeno, A. P. Mackenzie, H. Luetkens, C. W. Hicks, H. Klauss, arXiv:2001.08152.
- [13] J. Xia, Y. Maeno, P. T. Beyersdorf, M. M. Fejer, and A. Kapitulnik, *Phys. Rev. Lett.* **97**, 167002 (2006).
- [14] F. Kidwingira, J.D. Strand, D.J. van Harlingen, and Y. Maeno, *Science* **314**, 1267 (2006).
- [15] S. Ghosh, A. Shekhter, F. Jerzembeck, N. Kikugawa, D. A. Sokolov, M. Brando, A. P. Mackenzie, C. W. Hicks, B. J. Ramshaw, *Nat. Phys.* <https://doi.org/10.1038/s41567-020-1032-4> (2020).
- [16] S. Benhabib, C. Lupien, I. Paul, L. Berges, M. Dion, M. Nardone, A. Zitouni, Z.Q. Mao, Y. Maeno, A. Georges, L. Taillefer, C. Proust, *Nat. Phys.* <https://doi.org/10.1038/s41567-020-1033-3> (2020).
- [17] J-L. Zhang, Y. Li, W. Huang, and F-C. Zhang, *Phys. Rev. B* **102**, 180509(R) (2020).
- [18] D. Vollhardt and P. Wölfle, *The Superfluid Phases of Helium 3* (Dover Publications, New York, 1990).
- [19] A. Pustogow, Y. Luo, A. Chronister, Y. Su, D. A. Sokolov, F. Jerzembeck, A. P. Mackenzie, C. W. Hicks, N. Kikugawa, S. Raghu, E. D. Bauer, S. E. Brown, *Nature* **574**, 72 (2019).
- [20] K. Ishida, M. Manago, and Y. Maeno, *J. Phys. Soc. Jpn.* **89**, 034712 (2020).
- [21] K.D. Nelson, Z.Q. Mao, Y. Maeno, and Y. Liu, *Science* **306**, 1151 (2004).
- [22] J. Jang, D.G. Ferguson, V. Vakaryuk, R. Budakian, S.B. Chung, P.M. Goldbart, Y. Maeno, *Science* **331**, 186 (2011).
- [23] J. R. Kirtley, C. Kallin, C. W. Hicks, E. -A. Kim, Y. Liu, K. A. Moler, Y. Maeno, K. D. Nelson, *Phys. Rev. B* **76**, 014526 (2007).
- [24] C. W. Hicks, J. R. Kirtley, T. M. Lippman, N. C. Koshnick, M. E. Huber, Y. Maeno, W. M. Yuhasz, M. B. Maple, K. A. Moler, *Phys. Rev. B* **81**, 214501 (2010).
- [25] A. Chronister, A. Pustogow, N. Kikugawa, D. A. Sokolov, F. Jerzembeck, C.W. Hicks, A.P. Mackenzie, E.D. Bauer, S. E. Brown, arXiv:2007.13730, 2020.
- [26] J. F. Annett, G. Litak, B.L. Györfly, and K. I. Wysokiński, *Phys. Rev. B* **73**, 134501 (2006).
- [27] T. Scaffidi, J. C. Romers, and S. H. Simon, *Phys. Rev. B* **89**, 220510(R) (2014).

- [28] L.D. Zhang, W. Huang, F. Yang, and H. Yao, Phys. Rev. B **97**, 060510(R) (2018).
- [29] A. T. Rømer, D. D. Scherer, I. M. Eremin, P. J. Hirschfeld, and B. M. Andersen, Phys. Rev. Lett. **123**, 247001 (2019).
- [30] A. T. Rømer, D. D. Scherer, I. M. Eremin, P. J. Hirschfeld, and B. M. Andersen, Mod. Phys. Lett. B **34**, 2040052 (2020).
- [31] H. S. Roising, T. Scaffidi, F. Flicker, G. F. Lange, and S. H. Simon, Phys. Rev. Research **1**, 033108 (2019).
- [32] Z. Wang, X. Wang, and C. Kallin, Phys. Rev. B **101**, 064507 (2020).
- [33] N. Read and D. Green, Phys. Rev. B **61**, 10267 (2000).
- [34] E. Taylor, and C. Kallin, Phys. Rev. Lett. **108**, 157001 (2012).
- [35] K.I. Wysokiński, J. F. Annett, and B.L. Györfy, Phys. Rev. Lett. **108**, 077004 (2012).
- [36] Z. Wang, J. Berlinsky, G. Zwignagl, and C. Kallin, Phys. Rev. B **96**, 174511 (2017).
- [37] See the Supplementary Materials for details of the calculation of  $\sigma_H$  and  $\theta_K$ .
- [38] J. Xia, Y. Maeno, P.T. Beyersdorf, M. M. Fejer, and A. Kapitulnik, Phys. Rev. Lett. **97**, 167002 (2006).
- [39] M. Matsumoto and M. Sigrist, J. Phys. Soc. Jpn. **68**, 994 (1999).
- [40] A. Furusaki, M. Matsumoto and M. Sigrist, Phys. Rev. B **64**, 054514 (2001).
- [41] P.E.C. Ashby and C. Kallin, Phys. Rev. B **79**, 224509 (2009).
- [42] Y. Imai, K. Wakabayashi, and M. Sigrist, Phys. Rev. B **85**, 174532 (2012); Phys. Rev. B **88**, 144503 (2013).
- [43] S. Lederer, W. Huang, E. Taylor, S. Raghu, and C. Kallin, Phys. Rev. B **90**, 134521 (2014).
- [44] A. Bouhon and M. Sigrist, Phys. Rev. B **90**, 220511(R) (2014).
- [45] W. Huang, S. Lederer, E. Taylor, C. Kallin, Phys. Rev. B **91**, 094507 (2015).
- [46] T. Scaffidi and S.H. Simon, Phys. Rev. Lett. **115**, 087003 (2015).
- [47] M. Sigrist and K. Ueda, Rev. Mod. Phys. **63**, 239 (1991).
- [48] X. Wang, Z. Wang, and C. Kallin, Phys. Rev. B **98**, 094501 (2018).
- [49] S.A. Kivelson, A.C. Yuan, B.J. Ramshaw, and R. Thomale, npj Quantum Mater. **5**, 43 (2020).
- [50] A. N. Petsch, M. Zhu, M. Enderle, Z. Q. Mao, Y. Maeno, I. I. Mazin, S. M. Hayden, Phys. Rev. Lett. **125**, 217004 (2020).
- [51] W. Huang, Y. Zhou, and H. Yao, Phys. Rev. B **100**, 134506 (2019).
- [52] A. Ramires and M. Sigrist, Phys. Rev. B **100**, 104501 (2019).
- [53] S.O. Kaba, D. Sénéchal, Phys. Rev. B **100**, 214507 (2019).
- [54] C. M. Puetter and H. -Y. Kee, Europhys. Lett. **98**, 27010 (2012).
- [55] A.J. Leggett, Phys. Rev. Lett. **14**, 536 (1965).
- [56] P. Steffens, Y. Sidis, J. Kulda, Z. Q. Mao, Y. Maeno, I. I. Mazin, and M. Braden, Phys. Rev. Lett. **122**, 047004 (2019).
- [57] E. Pavarini and I. I. Mazin, Phys. Rev. B **74**, 035115 (2007).
- [58] C. W. Hicks, D. O. Brodsky, E. A. Yelland, *et al.*, Science **344**, 283 (2014).
- [59] A. Steppke, L. Zhao, M. E. Barber, T. Scaffidi, *et al.*, Science **355**, eaaf9398 (2017).
- [60] C. A. Watson, A. S. Gibbs, A. P. Mackenzie, C. W. Hicks, K. A. Moler, Phys. Rev. B **98**, 094521 (2018).
- [61] S. Yonezawa, T. Kajikawa, and Y. Maeno, J. Phys. Soc. Jpn. **83**, 083706.
- [62] Y. -S. Li, N. Kikugawa, D. A. Sokolov, F. Jerzembeck, A. S. Gibbs, Y. Maeno, C. W. Hicks, M. Nicklas, A.P. Mackenzie, arXiv:1906.07597.
- [63] T. Scaffidi, arXiv:2007.13769.
- [64] R. Gupta, T. Saunderson, S. Shallcross, M. Gradhand, J. Quintanilla, J. Annett, Phys. Rev. B **102**, 235203 (2020).
- [65] K. Deguchi, M. A. Tanatar, Z. Q. Mao, T. Ishiguro, and Y. Maeno, J. Phys. Jpn. Soc. **71**, 2839 (2002).
- [66] K. Deguchi, Z. Q. Mao, Y. Yaguchi, and Y. Maeno, Phys. Rev. Lett. **92**, 047002 (2004).
- [67] S. Yonezawa, T. Kajikawa, and Y. Maeno, Phys. Rev. Lett. **110**, 077003 (2013).
- [68] S. Nishizaki, Y. Maeno, and Z.Q. Mao, J. Phys. Soc. Jpn. **69**, 572 (2000).
- [69] I. A. Firmo, S. Lederer, C. Lupien, A. P. Mackenzie, J. C. Davis, and S.A. Kivelson, Phys. Rev. B **88**, 134521 (2013).
- [70] E. Hassinger, P. Bourgeois-Hope, *et al.*, Phys. Rev. X **7**, 011032 (2017).
- [71] John F. Dodaro, Zhiqiang Wang, and Catherine Kallin, Phys. Rev. B **98**, 214520 (2018).
- [72] D.F. Agterberg, T.M. Rice, and M. Sigrist, Phys. Rev. Lett. **78**, 3374 (1997).
- [73] M. E. Zhitomirsky and T. M. Rice, Phys. Rev. Lett. **87**, 057001 (2001).
- [74] A. Ramires and M. Sigrist, Phys. Rev. B **94**, 104501 (2016).
- [75] W-S. Wang, C-C. Zhang, F-C. Zhang, and Q-H. Wang, Phys. Rev. Lett. **122**, 027002 (2019).
- [76] O. Gingras, R. Nourafkan, A. -M. S. Tremblay, and M. Côté, Phys. Rev. Lett. **123**, 217005 (2019).
- [77] Y. Li and W. Huang, arXiv:1909.03141.
- [78] H. G. Suh, H. Menke, P. M. R. Brydon, C. Timm, A. Ramires, D. F. Agterberg, Phys. Rev. Research **2**, 032023 (2020).
- [79] W. Chen and J. An, Phys. Rev. B **102**, 094501 (2020).
- [80] A. W. Lindquist, H-Y. Kee, Phys. Rev. Research **2**, 032055 (2020).
- [81] A. Sumiyama, D. Kawakatsu, J. Gouchi, A. Yamaguchi, G. Motoyama, Y. Hirose, R. Settai, Y. Ōnuki, JPS Conf. Proc. **3**, 015017 (2014).
- [82] R. Willa, M. Hecker, R.M. Fernandes, J. Schmalian, arXiv:2011.01941.

# Supplemental Material for “On the possibility of mixed helical p-wave pairing in Sr<sub>2</sub>RuO<sub>4</sub>”

Wen Huang<sup>1</sup> and Zhiqiang Wang<sup>2</sup>

<sup>1</sup>Shenzhen Institute for Quantum Science and Engineering & Guangdong Provincial Key Laboratory of Quantum Science and Engineering, Southern University of Science and Technology, Shenzhen 518055, Guangdong, China

<sup>2</sup>James Franck Institute, University of Chicago, Chicago, Illinois 60637, USA

(Dated: November 3, 2021)

## CALCULATION OF THE ANOMALOUS HALL CONDUCTIVITY

In the absence of SOC, the two spin blocks decouple. We can calculate  $\sigma_H^\uparrow$  and  $\sigma_H^\downarrow$  separately.

### Spin up block

The model we consider consists of the two quasi-1d orbitals,  $d_{xz}$  and  $d_{yz}$ , of Sr<sub>2</sub>RuO<sub>4</sub>. Written in the basis  $\{c_{d_{xz}}(\mathbf{k}), c_{d_{yz}}(\mathbf{k})\}$  the spin up block of the normal state Hamiltonian is

$$\hat{H}_N(\mathbf{k}) \equiv \begin{pmatrix} \xi_{xz}(\mathbf{k}) & \lambda(\mathbf{k}) \\ \lambda(\mathbf{k}) & \xi_{yz}(\mathbf{k}) \end{pmatrix} = \begin{pmatrix} -2t \cos k_x - 2\tilde{t} \cos k_y - \mu & 4t' \sin k_x \sin k_y \\ 4t' \sin k_x \sin k_y & -2t \cos k_y - 2\tilde{t} \cos k_x - \mu \end{pmatrix}. \quad (1)$$

The corresponding BdG Hamiltonian is

$$\hat{H}_{\text{BdG}}^\uparrow(\mathbf{k}) = \begin{pmatrix} \hat{H}_N(\mathbf{k}) & \hat{\Delta}^{\uparrow\uparrow}(\mathbf{k}) \\ [\hat{\Delta}^{\uparrow\uparrow}]^\dagger(\mathbf{k}) & -[\hat{H}_N]^T(-\mathbf{k}) \end{pmatrix} \quad (2)$$

with

$$\hat{\Delta}^{\uparrow\uparrow}(\mathbf{k}) = -(\Delta_{A_{1u}} - \Delta_{A_{2u}}) \begin{pmatrix} \sin k_x & 0 \\ 0 & -i \sin k_y \end{pmatrix}, \quad (3)$$

which is effectively a (spinless) chiral  $p_x - ip_y$  order parameter. For simplicity we have considered only intra-orbital pairing while neglected any inter-orbital one. The pairing component between the  $d_{xz}$  and  $d_{yz}$  orbitals,  $\Delta_{11}^{\uparrow\uparrow}$ , transforms like  $k_x$  under the spatial  $D_{4h}$  group. Hence,  $\Delta_{11}^{\uparrow\uparrow}(\mathbf{k}) = [\mathbf{d}_k^{(x)} \cdot \boldsymbol{\sigma} i \sigma_2]_{\uparrow\uparrow} = -(\Delta_{A_{1u}} - \Delta_{A_{2u}}) \sin k_x$ , where  $\mathbf{d}_k^{(x)}$  is the  $k_x$ -like part of  $\mathbf{d}_k = \Delta_{A_{1u}}(\hat{x} \sin k_x + \hat{y} \sin k_y) + \Delta_{A_{2u}}(\hat{x} \sin k_y - \hat{y} \sin k_x)$ . Similarly,  $\Delta_{22}^{\uparrow\uparrow}(\mathbf{k}) = [\mathbf{d}_k^{(y)} \cdot \boldsymbol{\sigma} i \sigma_2]_{\uparrow\uparrow}$ . From  $H_{\text{BdG}}$  we define the electric current velocity operator

$$\hat{\mathbf{v}}(\mathbf{k}) = \begin{pmatrix} \nabla_{\mathbf{k}} \xi_{xz}(\mathbf{k}) & \nabla_{\mathbf{k}} \lambda(\mathbf{k}) \\ \nabla_{\mathbf{k}} \lambda(\mathbf{k}) & \nabla_{\mathbf{k}} \xi_{yz}(\mathbf{k}) \end{pmatrix} \otimes 1_{2 \times 2}, \quad (4)$$

where  $1_{2 \times 2}$  is the identity matrix in the Nambu particle-hole space.

We calculate  $\sigma_H^\uparrow$  using the standard one-loop Kubo formula

$$\sigma_H^\uparrow(\omega) = \frac{i}{\omega} \frac{\pi_{xy}(\mathbf{q} = 0, \omega + i0^+) - \pi_{yx}(\mathbf{q} = 0, \omega + i0^+)}{2}, \quad (5)$$

where  $\pi_{xy}(\mathbf{q}, i\nu_m)$  is the electric current-current density correlator, given by

$$\pi_{xy}(0, i\nu_m) = e^2 T \sum_n \sum_{\mathbf{k}} \text{Tr}[\hat{v}_x(\mathbf{k}) \hat{G}(\mathbf{k}, i\omega_n) \hat{v}_y(\mathbf{k}) \hat{G}(\mathbf{k}, i\omega_n + i\nu_m)]. \quad (6)$$

In this equation  $\hat{G}(\mathbf{k}, i\omega_n) \equiv [i\omega_n - \hat{H}_{\text{BdG}}^\uparrow(\mathbf{k})]^{-1}$  is the Green's function.  $\omega_n = (2n + 1)\pi T$  and  $\nu_m = 2m\pi T$  are Fermionic and Bosonic Matsubara frequencies. The trace Tr is with respect to both the Nambu particle-hole and orbital spaces.  $e$  is the charge of an electron. Using Eq. (2) in the expression of  $\pi_{xy}(0, i\nu_m)$  in Eq. (6), completing the Matsubara sum over  $\omega_n$ , and then making the analytical continuation,  $i\nu_m \rightarrow \omega + i\delta$ , we obtain

$$\frac{\sigma_H^\uparrow(\omega)}{e^2/\hbar} = \sum_{\mathbf{k}} \frac{\mathcal{F}_{\mathbf{k}}^\uparrow}{E_+^\uparrow(\mathbf{k})E_-^\uparrow(\mathbf{k})[E_+^\uparrow(\mathbf{k}) + E_-^\uparrow(\mathbf{k})][(E_+^\uparrow(\mathbf{k}) + E_-^\uparrow(\mathbf{k}))^2 - (\omega + i\delta)^2]}, \quad (7)$$

where

$$\mathcal{F}_{\mathbf{k}}^{\uparrow} = 32 (t - \tilde{t})(t')^2 (\Delta_1 - \Delta_2)^2 (\sin^2 k_x \cos k_y + \sin^2 k_y \cos k_x) \sin^2 k_x \sin^2 k_y. \quad (8)$$

$E_{\pm}^{\uparrow}(\mathbf{k})$  are eigenvalues of  $\hat{H}_{\text{BdG}}^{\uparrow}(\mathbf{k})$ .

$$E_{\pm}^{\uparrow} = \sqrt{\frac{-\alpha \pm \sqrt{\alpha^2 - 4\beta}}{2}}, \quad (9a)$$

$$\alpha = -(\xi_{xz}^2 + |\Delta_{11}^{\uparrow\uparrow}|^2 + \xi_{yz}^2 + |\Delta_{22}^{\uparrow\uparrow}|^2 + 2\lambda^2), \quad (9b)$$

$$\beta = (\xi_{xz}^2 + |\Delta_{11}^{\uparrow\uparrow}|^2)(\xi_{yz}^2 + |\Delta_{22}^{\uparrow\uparrow}|^2) + \lambda^4 + \lambda^2 (|\Delta_{11}^{\uparrow\uparrow}|^2 \Delta_{22}^{\uparrow\uparrow} + \Delta_{11}^{\uparrow\uparrow} |\Delta_{22}^{\uparrow\uparrow}|^2) - 2\lambda^2 \xi_{xz} \xi_{yz} \quad (9c)$$

For brevity we have suppressed the  $\mathbf{k}$  dependence in these equations.

Written out explicitly, the real and imaginary parts of  $\sigma_{\text{H}}^{\uparrow}$  are

$$\text{Re}[\sigma_{\text{H}}^{\uparrow}(\omega)] = \frac{e^2}{\hbar} \sum_{\mathbf{k}} \frac{\mathcal{F}_{\mathbf{k}}^{\uparrow}}{E_{+}^{\uparrow} E_{-}^{\uparrow} (E_{+}^{\uparrow} + E_{-}^{\uparrow}) [(E_{+}^{\uparrow} + E_{-}^{\uparrow})^2 - \omega^2]}, \quad (10)$$

$$\text{Im}[\sigma_{\text{H}}^{\uparrow}(\omega)] = \frac{e^2}{\hbar} \sum_{\mathbf{k}} \frac{\mathcal{F}_{\mathbf{k}}^{\uparrow}}{E_{+}^{\uparrow} E_{-}^{\uparrow}} \frac{\pi}{2\omega^2} \left[ \delta(\omega - (E_{+}^{\uparrow} + E_{-}^{\uparrow})) - \delta(\omega + (E_{+}^{\uparrow} + E_{-}^{\uparrow})) \right]. \quad (11)$$

### Spin down block

The derivation of  $\sigma_{\text{H}}^{\downarrow}$  is almost identical. The only difference is that in the definition of the BdG Hamiltonian,  $\hat{\Delta}^{\uparrow\uparrow}$  is now replaced by

$$\hat{\Delta}^{\downarrow\downarrow}(\mathbf{k}) = (\Delta_{A_{1u}} + \Delta_{A_{2u}}) \begin{pmatrix} \sin k_x & 0 \\ 0 & i \sin k_y \end{pmatrix}. \quad (12)$$

Correspondingly,

$$\frac{\sigma_{\text{H}}^{\downarrow}(\omega)}{e^2/\hbar} = \sum_{\mathbf{k}} \frac{\mathcal{F}_{\mathbf{k}}^{\downarrow}}{E_{+}^{\downarrow} E_{-}^{\downarrow} (E_{+}^{\downarrow} + E_{-}^{\downarrow}) [(E_{+}^{\downarrow} + E_{-}^{\downarrow})^2 - (\omega + i\delta)^2]} \quad (13)$$

with

$$\mathcal{F}_{\mathbf{k}}^{\downarrow} = -32(t - \tilde{t})(t')^2 (\Delta_1 + \Delta_2)^2 (\sin^2 k_x \cos k_y + \sin^2 k_y \cos k_x) \sin^2 k_x \sin^2 k_y. \quad (14)$$

The expressions of  $E_{\pm}^{\downarrow}$  are also almost identical to those of  $E_{\pm}^{\uparrow}$  in Eq. (9), except that  $\{\Delta_{11}^{\uparrow\uparrow}, \Delta_{22}^{\uparrow\uparrow}\}$  are now replaced with  $\{\Delta_{11}^{\downarrow\downarrow}, \Delta_{22}^{\downarrow\downarrow}\}$ . Although the gap magnitudes can be quite different for spin up and down,  $\min\{E_{+}^{\uparrow}(\mathbf{k}) + E_{-}^{\uparrow}(-\mathbf{k})\}$ , which determines the onset frequency of  $\text{Im}[\sigma_{\text{H}}^{\uparrow}(\omega)]$  (see Eq. (11)), is actually nearly the same as  $\min\{E_{+}^{\downarrow}(\mathbf{k}) + E_{-}^{\downarrow}(-\mathbf{k})\}$ , because both of them are governed by the orbital-hybridization parameter  $t'$  [1] instead of the pairing gap magnitudes. This explains why, in Fig. 1,  $\text{Im}[\sigma_{\text{H}}^{\uparrow}(\omega)]$  and  $\text{Im}[\sigma_{\text{H}}^{\downarrow}(\omega)]$  become nonzero essentially at the same frequency.

Comparing  $\mathcal{F}_{\mathbf{k}}^{\downarrow}$  to  $\mathcal{F}_{\mathbf{k}}^{\uparrow}$  in Eq. (8) we see that they carry opposite signs, leading to a partial cancellation between  $\sigma_{\text{H}}^{\downarrow}$  and  $\sigma_{\text{H}}^{\uparrow}$  (see Fig. 1). This sign difference comes from  $\hat{\Delta}^{\downarrow\downarrow}$  having a chirality opposite to that of  $\hat{\Delta}^{\uparrow\uparrow}$ . If we set either  $\Delta_{A_{1u}} = 0$  or  $\Delta_{A_{2u}} = 0$ , then  $\mathcal{F}_{\mathbf{k}}^{\uparrow} = -\mathcal{F}_{\mathbf{k}}^{\downarrow}$ ,  $E_{\pm}^{\uparrow}(\mathbf{k}) = E_{\pm}^{\downarrow}(\mathbf{k})$ , and  $\sigma_{\text{H}}^{\downarrow} + \sigma_{\text{H}}^{\uparrow} = 0$ , as we expect. Also, under the sign flip,  $\Delta_{A_{1u}} \rightarrow -\Delta_{A_{1u}}$  or  $\Delta_{A_{2u}} \rightarrow -\Delta_{A_{2u}}$ ,  $\sigma_{\text{H}}^{\uparrow} \leftrightarrow -\sigma_{\text{H}}^{\downarrow}$  so that  $\sigma_{\text{H}} \rightarrow -\sigma_{\text{H}}$ . This can be seen from Fig. 2, where we plot  $\sigma_{\text{H}}(\omega)$  for a given frequency as a function of  $4\Delta_{A_{1u}}\Delta_{A_{2u}}/(|\Delta_{A_{1u}}| + |\Delta_{A_{2u}}|)^2$ .  $\sigma_{\text{H}}$  changes its sign because flipping the sign of either  $\Delta_{A_{1u}}$  or  $\Delta_{A_{2u}}$  changes whether the spin-up  $p_x - ip_y$  or the spin-down  $p_x + ip_y$  pairing dominates.

### ESTIMATION OF THE KERR ANGLE

From the calculated  $\sigma_{\text{H}}(\omega)$  we can estimate the Kerr angle for  $\hbar\omega = 0.8\text{eV}$  using

$$\theta_{\text{K}}(\omega) = \frac{4\pi}{\omega d} \text{Im}\left[\frac{\sigma_{\text{H}}(\omega)}{n(n^2 - 1)}\right], \quad (15)$$

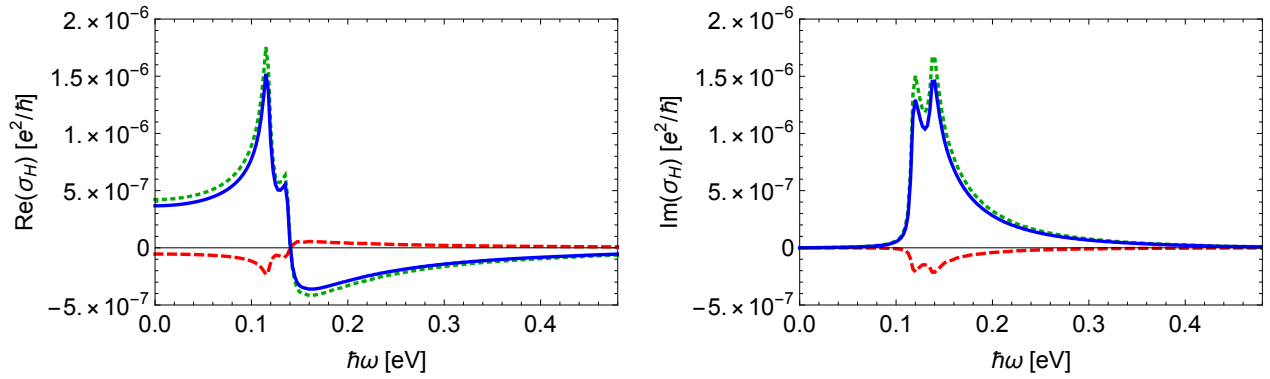


FIG. 1. Spin  $\uparrow$  (red dashed line),  $\downarrow$  (dark green dotted line), and the total (blue solid line) contributions to the  $T = 0$  Hall conductivity. Left:  $\text{Re}[\sigma_H]$ ; Right:  $\text{Im}[\sigma_H]$ . Band parameters used are [1]:  $t = \mu = 0.4 \text{ eV}$ ,  $\tilde{t} = 0.1t$ , and  $t' = 0.05t$ .  $\Delta_{A_{1u}} = 2\Delta_{A_{2u}} = \frac{2}{3}\Delta_{\text{max}}$  with  $\Delta_{\text{max}} = 0.23 \text{ meV}$  [1].

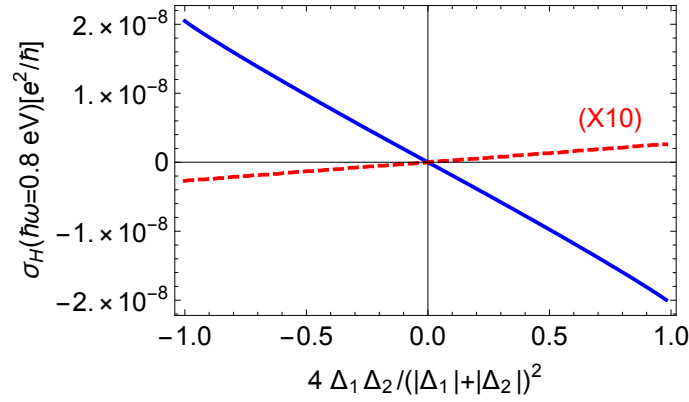


FIG. 2. Real (blue solid line) and imaginary (red dashed line) parts of the zero temperature  $\sigma_H(\omega)$  as a function of  $4\Delta_{A_{1u}}\Delta_{A_{2u}}/(|\Delta_{A_{1u}}| + |\Delta_{A_{2u}}|)^2$ .  $\hbar\omega = 0.8 \text{ eV}$ .  $\Delta_{\text{max}} = |\Delta_{A_{1u}}| + |\Delta_{A_{2u}}| = 0.23 \text{ meV}$  is kept a constant in this calculation. The plot shows that  $\sigma_H$  is roughly linear in  $4\Delta_{A_{1u}}\Delta_{A_{2u}}/(|\Delta_{A_{1u}}| + |\Delta_{A_{2u}}|)^2$ . From the plot we see that  $\sigma_H$  is odd in the relative sign between  $\Delta_{A_{1u}}$  and  $\Delta_{A_{2u}}$ , but even under the interchange  $|\Delta_{A_{1u}}| \leftrightarrow |\Delta_{A_{2u}}|$ .

where  $n = n(\omega)$  is the complex index of refraction, given by

$$n = \sqrt{\epsilon_{ab}(\omega)}, \quad (16)$$

$$\epsilon_{ab}(\omega) = \epsilon_{\infty} + \frac{4\pi i}{\omega} \sigma(\omega). \quad (17)$$

$\epsilon_{ab}(\omega)$  is the permeability tensor in the  $ab$ -plane.  $\epsilon_{\infty} = 10$  [1] is the background permeability.  $d = 6.8 \text{ \AA}$  is the inter-layer spacing along the  $c$ -axis.  $\sigma(\omega)$  is the optical longitudinal conductivity. Following Ref. [1] we use a simple Drude model for  $\sigma(\omega)$

$$\sigma(\omega) = -\frac{\omega_{\text{pl}}^2}{4\pi i(\omega + i\Gamma)}, \quad (18)$$

where  $\omega_{\text{pl}} = 2.9 \text{ eV}$  is the plasma frequency and  $\Gamma = 0.4 \text{ eV}$  is an elastic scattering rate. At  $\hbar\omega = 0.8 \text{ eV}$ ,  $\sigma(\omega) = 0.33 + i0.67$ ,  $\epsilon_{ab} = -0.52 + i5.20$ , and  $n = 1.53 + i1.69$ . Plugging this  $n$  value into Eq. (15) and using the  $\sigma_H(\hbar\omega = 0.8 \text{ eV})$  value from Fig. 2 we get  $\theta_K \approx 20 \text{ nrad}$ . The whole frequency dependence of  $\theta_K$  is shown in Fig. 3.

[1] E.Taylor, and C. Kallin, Phys. Rev. Lett. 108, 157001 (2012).

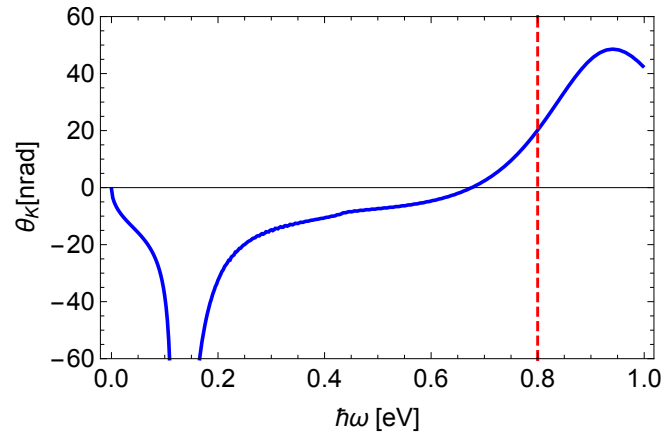


FIG. 3. (color online) Kerr angle as a function of  $\hbar\omega$ . Band parameters and the values of  $\{\Delta_{A_{1u}}, \Delta_{A_{2u}}\}$  are the same as in Fig. 1.